# Evaluation of charge penetration between distributed multipolar expansions

Mark A. Freitag, Mark S. Gordon, Jan H. Jensen, and Walter J. Stevens

# Evaluation of charge penetration between distributed multipolar expansions

Mark A. Freitag and Mark S. Gordon
*Department of Chemistry, Iowa State University, Ames, Iowa 50011*

Jan H. Jensen
*Department of Chemistry, University of Iowa, Iowa City, Iowa 52242*

Walter J. Stevens
*Physical and Chemical Properties Division (838), National Institute of Standards and Technology, Gaithersburg, Maryland 20899-8380*

A formula to calculate the charge penetration energy that results when two charge densities overlap has been derived for molecules described by an effective fragment potential (EFP). The method has been compared with the *ab initio* charge penetration, taken to be the difference between the electrostatic energy from a Morokuma analysis and Stone's Distributed Multipole Analysis. The average absolute difference between the EFP method and the *ab initio* charge penetration for dimers of methanol, acetonitrile, acetone, DMSO, and dichloromethane at their respective equilibrium geometries is 0.32 kcal mol$^{-1}$. © *2000 American Institute of Physics.* [S0021-9606(00)30817-0]

## I. INTRODUCTION

There are several fundamental long- and short-range intermolecular interactions that occur between closed shell molecules in their ground states: Long-range interactions ($U \propto r^{-n}$) are due to electrostatics, polarization, and dispersion; while exchange repulsion, charge transfer, and charge penetration are considered to be short-range ($U \propto e^{-\alpha r}$).[1] In principle, one can calculate all these interactions to a desired level of accuracy from the system's approximate wave function using *ab initio* techniques. In practice, the computational demands of such calculations quickly become insurmountable as the size of the system increases. This is a particularly difficult problem when one wishes to study solvated species, and so in recent years there has been considerable work in developing discrete potentials, given in terms of the above intermolecular interactions, for common solvents, particularly water.[2] The goal in these studies is to develop a pseudo-quantum potential that can recover *ab initio* results while requiring minimal CPU time.

One such effort has been the development of the Effective Fragment Potential (EFP) method.[3] In this method, one typically divides the total system into two parts, an *ab initio*, or active region, and a fragment region (although there is no explicit need for an *ab initio* region). Then the fragment–fragment and/or fragment-*ab initio* interactions are calculated within the framework of the EFP methodology. Since the EFP model to date has been based on Hartree–Fock theory, EFPs allow for the calculation of those intermolecular interactions that one would expect to find at the Hartree–Fock level of theory: Electrostatics, polarization, exchange repulsion/charge transfer, and charge penetration.

In several recent papers a modification of the original EFP method has been discussed,[4] the key feature of which is the method's generalization to *any* solvent. This discussion is continued in the present work with a focus on the calculation of fragment–fragment charge penetration.

Conceptually, charge penetration can be understood in the following way: Consider two molecules separated by a large distance from one another in space. The electrostatic interaction between these two species is then very well represented by Stone's distributed multipolar analysis (DMA),[5] in which the electrostatic potential of each molecule is expanded about several points, typically the atom centers and bond midpoints, into monopoles, dipoles, quadrupoles, octopoles, etc.[6] The interaction energy is then calculated using the expressions for classical multipolar interactions. However, if the two molecules are brought close enough, such that their charge densities overlap, the nuclei on one molecule will no longer be shielded by its own electron density, and will experience a greater attraction for the electron density associated with the other species. The energy difference resulting from this increased attraction is referred to as charge penetration.

Mathematically, Stone demonstrated the origin of charge penetration through the following simple example:[1] Consider the interaction of a hydrogenlike atom with nuclear charge $Z$ and a proton. The wave function of the former is given by

$$\psi(r) = \left( \frac{Z^3}{\pi} \right)^{1/2} e^{-Zr} \tag{1}$$

and the electron charge density is given by

$$\rho(r) = -\frac{Z^3}{\pi} e^{-2Zr}. \tag{2}$$

One can then use Poisson's equation ($\nabla^2 V = -(\rho/\varepsilon_0)$), where $\varepsilon_0$ is the permittivity of free space, to find the potential due to that density. This results in

$$V(r) = -\frac{1}{r} + e^{-2Zr}\left(Z + \frac{1}{r}\right). \tag{3}$$

Since a multipolar expansion is in essence a Taylor expansion of the potential, which is a simple function of $1/r$, the second term in Eq. (3) is identified as the charge penetration. At moderate distances, the charge penetration falls off as a simple exponential.

It is well known that the exchange repulsion decays exponentially with distance. Murrell and Teixeira-Dias[7] have shown that charge penetration ($E^{\text{pen}}$) and exchange repulsion energies ($E^{\text{XR}}$) behave similarly, and have suggested the following relation between the two:

$$E^{\text{XR}} = -E^{\text{pen}}(a + bR), \tag{4}$$

where $a$ and $b$ are empirical parameters, and $R$ is the intermolecular separation. Conceptually, charge penetration should also be related to the intermolecular overlap. Murrell had earlier observed that

$$E^{\text{XR}} = \frac{kS^2}{R}, \tag{5}$$

where $k$ is an empirical parameter and $S$ is the overlap integral between two molecular wave functions. Taken together, Eqs. (4) and (5) suggest that $E^{\text{pen}}$ roughly scales as the square of the intermolecular overlap. This suggestion is supported by a recently published equation[8] for $E^{\text{pen}}$ between two nonorthogonal MOs $i$ and $j$,

$$E_{ij}^{\text{pen}} = -2\left(\frac{1}{-2\ln S_{ij}}\right)^{1/2}\frac{S_{ij}^2}{R_{ij}}, \tag{6}$$

where $R_{ij}$ is the distance between Gaussian centers. Equation (6) is derived within the Spherical Gaussian Overlap[9] approximation, and yields charge penetration energies that are, on average, within 0.25 kcal mol$^{-1}$ (Ref. 10) of the exact result for six different homomolecular dimers of common solvents.[8]

An alternative, presumably less computationally demanding, way to calculate charge penetration between fragments is to introduce a damping function that multiplies the electrostatic potential. Consider Eq. (3), when rewritten as[1]

$$V(r) = [1 - e^{-2Zr}(1 + rZ)]\left[-\frac{1}{r}\right] = f^{\text{damp}}(r)V^{\text{mult}}(r). \tag{7}$$

This suggests that a multipole expansion of the electrostatic potential ($V^{\text{mult}}$) can be corrected for charge penetration effects by using a damping function, $f^{\text{damp}}$. Indeed, as part of the original EFP method, Day *et al.* have used a damping function to model the electrostatic charge penetration between a distributed multipole expansion and an *ab initio* charge density.[3] Damping functions have also been used to correct multipolar expansion models of the induction energy,[11] and dispersion energy.[12]

The present paper describes the use of damping functions to model charge penetration effects between two or more multipole expansions, i.e., to correct the DMA electrostatic interactions between EFPs. The basic procedure is as follows: One must choose the parameter in the damping function such that the function fits the molecular *ab initio*
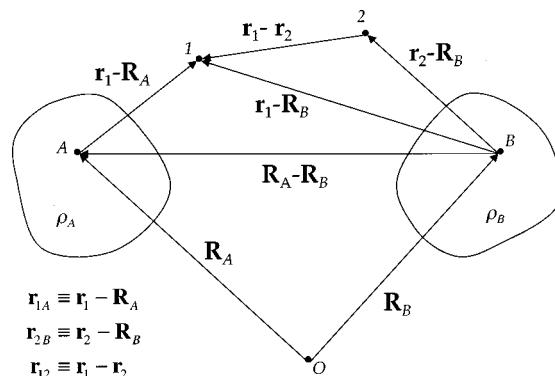


FIG. 1. Notation used in Sec. II. (See text for explanation.)

electrostatic potential well in the region of interest. Then the difference between the damped and undamped electrostatic interactions, within the framework of the DMA, will be a good approximation to the charge penetration. A derivation of this EFP/EFP charge penetration energy, along with an explanation of how the damping function parameter is found, is given in Sec. II. The success of this method for several homomolecular dimers is demonstrated in Sec. III. A summary of our findings is presented in Sec. IV. The entire procedure described here has been implemented in the electronic structure code GAMESS.[13]

## II. THEORY

The notation used in the following equations is defined in Fig. 1. The charge densities $\rho_A$ and $\rho_B$ are centered at points $A$ and $B$, respectively. These points represent the atomic centers and bond midpoints for EFPs. Points 1 and 2 represent electronic positions associated with $\rho_A$ and $\rho_B$, respectively. All points are referenced from an arbitrary origin, $O$. Using these definitions, the electrostatic interaction of two charge densities $\rho_A$ and $\rho_B$ is given by

$$E^{\text{Elec}} = \int\int d\mathbf{r}_1 d\mathbf{r}_2 \rho_A(\mathbf{r}_{1A})\rho_B(\mathbf{r}_{2B})|\mathbf{r}_{12}|^{-1}$$

$$= \int d\mathbf{r}_1 \rho_A(\mathbf{r}_{1A})\int d\mathbf{r}_2 \rho_B(\mathbf{r}_{2B})|\mathbf{r}_{12}|^{-1}, \tag{8}$$

where $\mathbf{r}_{1A} = \mathbf{r}_1 - \mathbf{R}_A$. In the EFP method the electrostatic potential due to the charge density is expanded in terms of charges, dipoles, quadrupoles, and octupoles at each atomic center and bond midpoint using Stone's distributed multipolar analysis:

$$E^{\text{Elec}} = \int d\mathbf{r}_1 \rho_A(\mathbf{r}_{1A})\int d\mathbf{r}_2 \rho_B(\mathbf{r}_{2B})\left[|\mathbf{r}_{1B}|^{-1}\right.$$

$$\left. -\frac{(\mathbf{r}_{12} - \mathbf{r}_{1B})\mathbf{r}_{1B}}{r_{1B}^3} + \cdots\right]$$

$$= \int d\mathbf{r}_1 \rho_A(\mathbf{r}_{1A})V_B^{\text{mult}}(\mathbf{r}_{1B}), \tag{9}$$

where, as suggested by Eq. (9), $V_B^{\text{mult}}$ is expanded in multipolar terms:

$$V_B^{\text{mult}}(\mathbf{r}_{1B}) = V_B^{\text{charge}}(\mathbf{r}_{1B}) + V_B^{\text{dipole}}(\mathbf{r}_{1B}) + \cdots. \tag{10}$$

Then, as indicated above, the effect of charge penetration is accounted for by multiplying Eq. (10) by a damping function. This damping function should have a number of features: (a) go to unity for large $R_{AB}$ and fall off toward zero as $R_{AB}$ approaches zero (where $R_{AB}$ is the distance between points $A$ and $B$); (b) fit well to the *ab initio* electrostatic potential of an isolated fragment in a region near its van der Waals radius; and (c) give rise to tractable integrals in Eq. (9). After numerous tests with many functions that fit one or more of these criteria, it was found that a simple exponential function gave the best balance of the desired qualities:

$$\tilde{V}_A^{\text{mult}}(\mathbf{r}_{1A}) = (1 - e^{-\alpha_A r_{1A}}) V_A^{\text{mult}}(\mathbf{r}_{1A}). \tag{11}$$

The parameter $\alpha$ is determined by minimizing the difference, $\Delta$, between the quantum mechanical electrostatic potential ($ES$) and the multipolar expansion of the potential over a grid of points:

$$\Delta = \sum_{\text{grid points}} [V_{ab\ initio}^{ES} - V_{\text{damped multipole}}^{ES}]^2.$$

To account for the fact that two damped distributed multipolar expansions are interacting, the charge density on $A$, $\rho_A(\mathbf{r}_{1A})$, is found by applying Poisson's equation to the damped charge potential, Eq. (11):

$$\rho_A(\mathbf{r}_{1A}) = -\varepsilon_0 \nabla^2 \tilde{V}_A^{\text{mult}}(\mathbf{r}_{1A}) = \rho_A^{\text{charge}}(\mathbf{r}_{1A}) + \rho_A^{\text{dipole}}(\mathbf{r}_{1A})$$
$$+ \cdots. \tag{12}$$

Since Poisson's equation is applied to each term in the damped charge electrostatic potential, the charge density is also expressed in terms of charge, dipole, quadrupole, etc., contributions. Then using Eqs. (12) and (10), the integral in Eq. (9) becomes

$$\tilde{E}^{\text{Elec}} = \int d\mathbf{r}_1 \rho_A(\mathbf{r}_{1A}) \tilde{V}_B^{\text{mult}}(\mathbf{r}_{1B})$$

$$= \int d\mathbf{r}_1 [\rho_A^{\text{charge}}(\mathbf{r}_{1A}) + \rho_A^{\text{dipole}}(\mathbf{r}_{1A}) + \cdots]$$

$$\times [\tilde{V}_B^{\text{charge}}(\mathbf{r}_{1B}) + \tilde{V}_B^{\text{dipole}}(\mathbf{r}_{1B}) + \cdots]. \tag{13}$$

Consider the first integral in Eq. (13):

$$\tilde{E}_{\text{chg-chg}}^{\text{Elec}} \approx \int d\mathbf{r}_1 \rho_A^{\text{charge}}(\mathbf{r}_{1A}) \tilde{V}_B^{\text{charge}}(\mathbf{r}_{1B}). \tag{14}$$

The approximate equality in Eq. (14) is due to the fact that it is not symmetric with respect to interchange of points $A$ and $B$. In Eq. (14), the charge density on $A$ interacts with the damped charge potential on $B$. If the points are interchanged, the charge density on $B$ interacts with the damped charge potential on $A$. Since we wish to calculate, e.g., charge–charge, charge–dipole, dipole–charge, etc., interactions separately, the integrals must be symmetrized with respect to interchange of points. This is done by adding the interchanged integral and taking a simple average of the resulting energies; for example,

$$\tilde{E}_{\text{chg-chg}}^{\text{Elec}} = \frac{1}{2} \left[ \int d\mathbf{r}_1 \rho_A^{\text{charge}}(\mathbf{r}_{1A}) \tilde{V}_B^{\text{charge}}(\mathbf{r}_{1B}) \right.$$

$$\left. + \int d\mathbf{r}_1 \rho_B^{\text{charge}}(\mathbf{r}_{1B}) \tilde{V}_A^{\text{charge}}(\mathbf{r}_{1A}) \right]. \tag{15}$$

For clarity, only the integral Eq. (14) will be explicitly discussed; the second term in Eq. (15) can be found trivially at the end of the derivation by exchanging points $A$ and $B$.

From Eqs. (10), (11), and (12) one finds

$$\rho_A^{\text{charge}}(\mathbf{r}_{1A}) = \frac{q_A \alpha_A^2 \varepsilon_0}{r_{1A}} e^{-\alpha_A r_{1A}}, \tag{16}$$

$$\tilde{V}_B^{\text{charge}}(\mathbf{r}_{1B}) = [1 - e^{-\alpha_B r_{1B}}] q_B r_{1B}^{-1}, \tag{17}$$

where the charge at point $A$, $q_A$, is found using Stone's method,[5] and $\varepsilon_0$ is the permittivity of free space.[1] Then Eq. (14) becomes

$$\tilde{E}_{\text{chg-chg}}^{\text{Elec}} \approx q_A q_B \alpha_A^2 \varepsilon_0 \left[ \int d\mathbf{r}_1 \frac{e^{-\alpha_A r_{1A}}}{r_{1A} r_{1B}} \right.$$

$$\left. - \int d\mathbf{r}_1 \frac{e^{-\alpha_A r_{1A}} e^{-\alpha_B r_{1B}}}{r_{1A} r_{1B}} \right], \tag{18}$$

which can be evaluated using the method described by Coulson[14] to yield

$$\tilde{E}_{\text{chg-chg}}^{\text{Elec}} \approx \frac{q_A q_B}{R_{AB}} \left[ 1 - e^{-\alpha_A R_{AB}} \right.$$

$$\left. - \frac{\alpha_A^2}{(\alpha_A^2 - \alpha_B^2)} [e^{-\alpha_B R_{AB}} - e^{-\alpha_A R_{AB}}] \right] \tag{19}$$

when $\alpha_A \neq \alpha_B$, and

$$\tilde{E}_{\text{chg-chg}}^{\text{Elec}} \approx \frac{q_A q_B}{R_{AB}} \left[ 1 - e^{-\alpha R_{AB}} \left( 1 + \frac{\alpha R_{AB}}{2} \right) \right] \tag{20}$$

when $\alpha_A = \alpha_B = \alpha$. In deriving Eqs. (19) and (20), we have used the fact that $4\pi\varepsilon_0 = 1$ in atomic units, and $R_{AB}$ represents the distance between expansion points $A$ and $B$.

A similar procedure is used to calculate electron-nuclear interactions; here the damped monopole contribution to the density is allowed to interact with the unscreened nuclear charge. Again, starting from Eq. (9), the interaction is given by

$$E_{\text{chg}}^{\text{Elec-Nuc}} = \int d\mathbf{r}_1 \rho_A^{\text{charge}}(\mathbf{r}_{1A}) Z_B r_{1B}^{-1}$$

$$+ \int d\mathbf{r}_1 \rho_B^{\text{charge}}(\mathbf{r}_{1B}) Z_A r_{1A}^{-1}$$

$$= q_A Z_B \alpha_A^2 \int d\mathbf{r}_1 \frac{e^{-\alpha_A r_{1A}}}{r_{1A} r_{1B}}$$

$$+ q_B Z_A \alpha_B^2 \int d\mathbf{r}_1 \frac{e^{-\alpha_B r_{1B}}}{r_{1A} r_{1B}}$$

$$= \frac{q_A Z_B}{R_{AB}} [1 - e^{-\alpha_A R_{AB}}] + \frac{q_B Z_A}{R_{AB}} [1 - e^{-\alpha_B R_{AB}}]. \tag{21}$$

J. Chem. Phys., Vol. 112, No. 17, 1 May 2000

Charge penetration      7303

Note that Eq. (21) is already symmetric with respect to interchange of $A$ and $B$. Finally, summing Eqs. (19) and (21), including the symmetrization, and subtracting out the undamped interactions, the charge penetration energy for charge–charge interactions only becomes

$$E_{chg-chg}^{Pen}$$

$$= -\frac{1}{2R_{AB}}$$

$$\times \left[ \begin{array}{l} q_A(q_B+2Z_B)e^{-\alpha_A R_{AB}}+q_B(q_A+2Z_A)e^{-\alpha_B R_{AB}} \\ +\dfrac{q_A q_B(\alpha_A^2+\alpha_B^2)}{\alpha_A^2-\alpha_B^2}(e^{-\alpha_B R_{AB}}-e^{-\alpha_A R_{AB}}) \end{array} \right],$$

$$(22)$$

where $\alpha_A \neq \alpha_B$ and $Z_{A,B}=0$ for bond midpoints. For the $\alpha_A=\alpha_B=\alpha$ case,

$$E_{chg-chg}^{Pen}=-\frac{1}{R_{AB}}\left[q_A q_B\left(1+\frac{\alpha R_{AB}}{2}\right) \right.$$

$$\left. +q_A Z_B+q_B Z_A \right]e^{-\alpha R_{AB}}. \qquad (23)$$

Note in Eqs. (22) and (23) the total charge penetration is the sum of all charge penetration energies between unique pairs of intermolecular DMA points $A$ and $B$.

If one follows the above procedures for charge–dipole interactions, an equation analogous to Eq. (13) is found:

$$\int d\mathbf{r}_1 \rho_A^{charge}(\mathbf{r}_{1A})\widetilde{V}_B^{dipole}(\mathbf{r}_{1B})$$

$$= q_A \mu_B \alpha_A^2 \varepsilon_0 \left[ \int d\mathbf{r}_1 \frac{e^{-\alpha_A r_{1A}}}{r_{1A}r_{1B}^2}\cos\theta_B \right.$$

$$\left. +\int d\mathbf{r}_1 \frac{e^{-\alpha_A r_{1A}}e^{-\alpha_B r_{1B}}}{r_{1A}r_{1B}^2}\cos\theta_B \right]. \qquad (24)$$

The integrals in Eq. (24) can also be evaluated analytically using Coulson's method, however, the first two dipole–charge integrals,

$$\int d\mathbf{r}_1 \rho_A^{dipole}(\mathbf{r}_{1A})\widetilde{V}_B^{charge}(\mathbf{r}_{1B})$$

$$= q_B \mu_A \alpha_A \varepsilon_0 \left[ \begin{array}{l} 2\displaystyle\int d\mathbf{r}_1 \dfrac{e^{-\alpha_A r_{1A}}\cos\theta_A}{r_{1A}^3 r_{1B}}-2 \\ \times \displaystyle\int d\mathbf{r}_1 \dfrac{e^{-\alpha_A r_{1A}}e^{-\alpha_B r_{1B}}\cos\theta_A}{r_{1A}^3 r_{1B}} \\ +\alpha_A \displaystyle\int d\mathbf{r}_1 \dfrac{e^{-\alpha_A r_{1A}}\cos\theta_A}{r_{1A}^2 r_{1B}}-\alpha_A \\ \times \displaystyle\int d\mathbf{r}_1 \dfrac{e^{-\alpha_A r_{1A}}e^{-\alpha_B r_{1B}}\cos\theta_A}{r_{1A}^2 r_{1B}} \end{array} \right], \qquad (25)$$

do not converge analytically. The resulting increase in CPU time rules out a numerical analysis of these integrals, and evaluating charge–dipole interactions without dipole–charge means not including all terms of a given order. Since this is undesirable as well, the following analysis includes only charge–charge interactions. It will be shown that even with such a seemingly severe truncation, a major percentage of the total charge penetration is still recovered.

Before the results of the above analysis are given, the procedure for determining the alpha parameter in the damping function will be briefly described. Consider the error function

$$\Delta = \sum_{\text{grid point}} [V_{ab\ initio}^{ES} - V_{damped\ multipole}^{ES}]^2, \qquad (26)$$

based on the difference between the *ab initio* and multipolar electrostatic potentials. A grid is defined about an isolated fragment molecule in the following manner: Concentric spheres are placed about each of the atom centers at 67% and
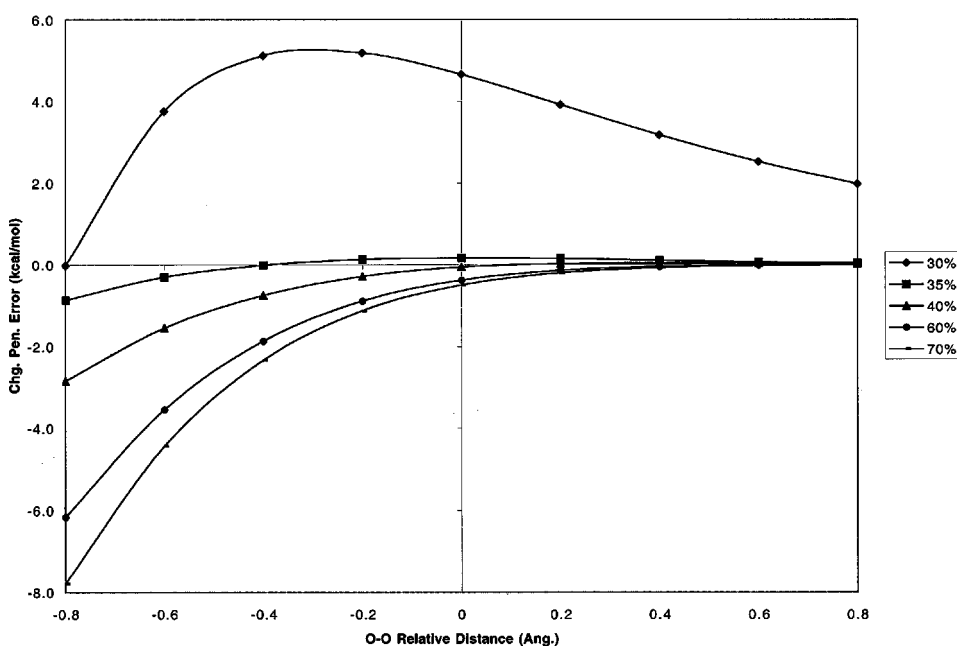


FIG. 2. Charge penetration error in kcal mol$^{-1}$ as a function of oxygen–oxygen distance in the water dimer, and as a function of $r_{min}$ (separate curves). $r_{max}$ is 300% of the Van der Waals radius of each atom.
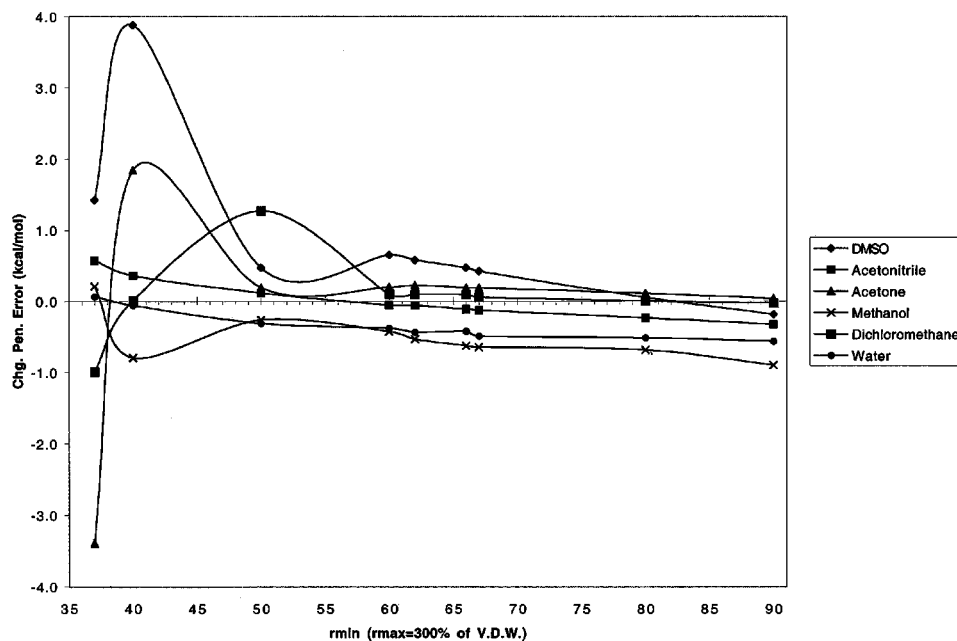
FIG. 3. Charge penetration error in kcal mol$^{-1}$ for six homomolecular dimers at their equilibrium geometries, as described in the text. The charge penetration error is given as a function of $r_{min}$. $r_{max}=300\%$ of the Van der Waals radius on each atom.

300% of the van der Waals radius of the corresponding atom. As will be shown in the next section, these values were chosen because they result in the best fit of the damping function to the *ab initio* density, and they were found to describe the physically most important regions in terms of charge penetration. The fragment is then placed within a three-dimensional Cartesian grid with a spacing of 0.50 Bohr in each direction, and any point not within the two spheres is discarded. It was found that the spacing has little effect on the fit unless the distance between grid points becomes too large; 0.50 Bohr balances run time and accuracy well. The *ab initio* density is calculated on the fragment during a GAMESS run, and the electrostatic potential is computed at each grid point. Finally, the parameter $\alpha$ is optimized in the exponential damping function such that $\Delta$ in Eq. (26) is minimized. Note that $\alpha$ is a property of the isolated monomer molecule.

## III. RESULTS AND DISCUSSION

Several tests were run to determine the optimal values of $(r_{min}/r_{max})$ for the radii of the concentric spheres about each atom to determine the set grid of points used in Eq. (19). Figure 2 shows the results on the water dimer using charge–charge interactions only. The dimer geometry used here was obtained by first finding the *ab initio* geometry at the RHF/6-31+G($d,p$) level of theory, and then superimposing the individual fragment monomer geometries on the dimer
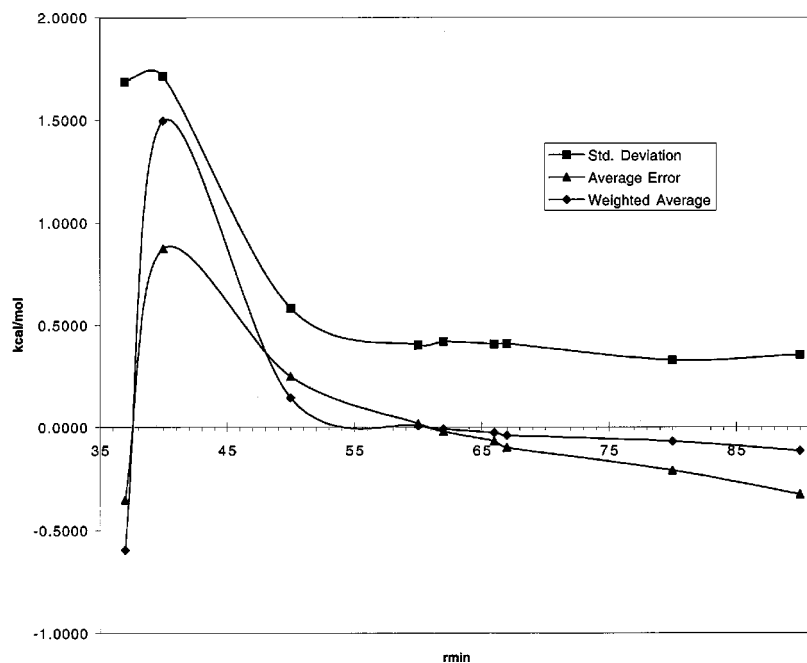


FIG. 4. The average error, standard deviation, and weighted average of the six homomolecular dimers in Fig. 3, as described in the text. The charge penetration error is given as a function of $r_{min}$. $r_{max}=300\%$ of the Van der Waals radius on each atom.

J. Chem. Phys., Vol. 112, No. 17, 1 May 2000

Charge penetration     7305

TABLE I. Charge penetration results, $6\text{-}31+\text{G}(d,p)$, for dimers of six common solvents; $r_{min}/r_{max}=67\%/300\%$ of van der Waals radius on each atom.[a]

| Dimer | Electrostatic energies | | | | |
| | Morokuma | FRAGONLY | Difference | Charge–charge | Error |
|---|---|---|---|---|---|
| $(CH_3)_2SO$ | −10.89 | −8.42 | −2.47 | −2.89 | 0.42 |
| $CH_3CN$ | −5.12 | −4.22 | −0.90 | −0.78 | −0.12 |
| $(CH_3)_2CO$ | −3.26 | −2.66 | −0.59 | −0.78 | 0.19 |
| $CH_3OH$ | −8.12 | −6.89 | −1.23 | −0.59 | −0.65 |
| $CH_2Cl_2$ | −1.74 | −1.47 | −0.28 | −0.33 | −0.06 |
| $H_2O$ | −8.21 | −7.12 | −1.09 | −0.60 | −0.49 |

[a]Grid spacing$=0.50$ Bohr. All values are in kcal mol[1]. The average absolute error is 0.32 kcal mol[1]. See text for discussion.

structure.[8] The abscissa is the relative distance between the water molecules; 0 Å represents the equilibrium distance between the oxygen atoms, negative values bring the fragments closer together, positive values move them further apart along a line connecting the oxygen atoms.

The fragment geometries described above are used for the Morokuma analysis $[6\text{-}31+\text{G}(d,p)]$, and the resulting electrostatic energies are taken to be the exact interactions for *ab initio* electronic densities. The FRAGONLY electrostatic energies are obtained from a fragment-only calculation on the dimer, and do not include any damping in the DMA. The difference between the Morokuma analysis and the FRAGONLY run is then taken to be the charge penetration that the present method is meant to calculate. It has been shown that a simple model of undamped electrostatics and hard spheres leads to a good prediction of equilibrium geometries for Van der Waals complexes,[15] so only the relevant interaction energies, with and without charge penetration, are reported here. In Fig. 2, $r_{max}$ is set at 300% of the Van der Waals radius of each atom, and $r_{min}$ is varied from 30% to 70% of the Van der Waals radius. The ordinate is the difference between our calculated charge penetration and the exact (Morokuma-FRAGONLY) charge penetration.

As $r_{min}$ approaches the atomic nuclei, the simplistic exponential damping function breaks down as evidenced by the large error for the $r_{min}=30\%$ curve. To understand this, consider the functional form of Stone's estimate of charge penetration given by the second term of Eq. (3) versus a simple exponential. The single parameter exponential function crosses the ordinate at unity when $r=0$, whereas Stone's function rises toward infinity. Therefore the exponential function does not contain adequate flexibility to fit the *ab initio* potential in this region close to the nuclear cusp. Depending on the specific monomer potential being fit, a breakdown is expected to occur somewhere in this region. Once this region has been entered, the alpha fitting procedure for the simple exponential quickly deteriorates, the foundation of the method erodes and results in unpredictable error in the calculated charge penetration. This can be seen in Fig. 3 for other dimers, where the average breakdown point occurs in the region of $r_{min}=55\%-60\%$. Referring back to Fig. 2: For the higher values of $r_{min}$ as the monomers move farther apart the charge penetration, and thus the error, goes to zero. At roughly $r_{min}=40\%$, almost all of the charge penetration is

TABLE II. Values of the alpha parameter used for the monomers that make up the dimers in Table I.[a]

| Monomer | DMA point | Alpha |
|---|---|---|
| $(CH_3)_2SO$ | C | 2.91 |
| | H | 1.66 |
| | S | 1.82 |
| | O | 1.94 |
| | S-C bm | 1.22 |
| | S-O bm | 10.00 |
| | C-H bm | 1.49 |
| $CH_3CN$ | C(methyl) | 2.17 |
| | C (cyano) | 1.96 |
| | N | 1.81 |
| | H | 1.76 |
| | C-N bm | 1.48 |
| | C-C bm | 0.56 |
| | C-H | 1.54 |
| $(CH_3)_2CO$ | C (methyl) | 1.89 |
| | C (carboxyl) | 1.75 |
| | O | 1.97 |
| | H | 1.75 |
| | C-O bm | 1.57 |
| | C-C bm | 1.03 |
| | C-H bm | 2.08 |
| $CH_3OH$ | C | 9.87 |
| | O | 1.93 |
| | H (methyl) | 1.65 |
| | H (hydroxyl) | 3.06 |
| | C-H bm | 1.63 |
| | C-O bm | 10.00 |
| | O-H bm | 10.00 |
| $CH_2Cl_2$ | C | 10.00 |
| | Cl | 1.78 |
| | H | 1.76 |
| | C-H bm | 2.00 |
| | C-Cl bm | 10.00 |
| $H_2O$ | O | 1.88 |
| | H | 2.95 |
| | O-H bm | 10.00 |

[a]The abbreviation ''bm'' refers to bond mid-point.

recovered at the equilibrium water dimer geometry, although we have seen that this value is most likely too close to the nuclear center to be used in general.

Tests on solvents other than water are shown in Fig. 3. It should be noted that although these tests were done on dimers of identical monomers, the method does not require this restriction; the charge penetration between *any* types of fragments can be found this way. The geometries were found using the same method as described above for water dimer. The Morokuma analysis was also performed using the $6\text{-}31 +\text{G}(d,p)$ basis. Again we note that at smaller values of $r_{min}$ the absolute error in all of the dimers increases unpredictably. As $r_{min}$ increases to a range of 60%–80%, the error becomes more stable, and as $r_{min}$ increases further, outside of the physically meaningful region for charge penetration, the error increases again for most dimers. One could find an optimal value of $r_{min}$ for each of the dimers shown, but overall the best choice seems to be in the range 60%–80%. Figure 4 shows the average error of the six dimers, the standard

deviation, and the average error weighted against the standard deviation. This plot shows where the standard deviation is both small and centered about zero error. Although this plot suggests the optimal value of $r_{min}$ is 60%, the weighted average difference between $r_{min}=60\%$ and 67% is only 0.05 kcal mol$^{-1}$, so very little is lost by choosing the larger, more conservative value of $r_{min}=67\%$. This choice is merely a suggestion based on the six dimers tested, and can be changed in GAMESS by the user. Table I shows the numerical results when $r_{min}=67\%$. The average absolute error is 0.32 kcal mol$^{-1}$; the largest absolute error is 0.65 kcal mol$^{-1}$ for methanol. If $r_{min}=80\%$, the average absolute error for these six dimers is reduced to 0.27 kcal mol$^{-1}$; however, this value of $r_{min}$ seems too high, since it nears the Van der Waals radius and the error is not spread as evenly about zero. Note that only the absolute value of the error is important. The overall charge penetration itself is attractive and thus negative, but there is no assurance that the charge penetration will not be overestimated using this method. This is especially true since only charge–charge interactions are included.

The values of alpha for $r_{min}=67\%$ are given in Table II. Note that since $\alpha$ is found by fitting the isolated monomer, these values will not change when used in heteromolecular fragment systems.

## IV. SUMMARY AND CONCLUSIONS

A formula to calculate the charge penetration energy that results when two charge densities overlap has been derived for molecules described by an effective fragment potential (EFP). The method has been compared with the *ab initio* charge penetration, taken to be the difference between the electrostatic energy from a Morokuma analysis and Stone's Distributed Multipole Analysis. The average absolute difference between the EFP method and the *ab initio* charge penetration for dimers of water, methanol, acetonitrile, acetone, DMSO, and dichloromethane at their equilibrium geometry is 0.32 kcal mol$^{-1}$.

The EFP method in general has been shown to reproduce *ab initio* results very accurately for water,[16] and this work is another step in the continuing development of a general EFP method that will accurately model *any* solvent. The derivation and implementation of dispersion and a parameter-free charge transfer in the EFP will be the subjects of future work.

[1] A. J. Stone, *The Theory of Intermolecular Forces* (Oxford University Press, Oxford, 1996).
[2] See, for example, Ref. 1, pp. 175–178, and references therein.
[3] P. N. Day, J. H. Jensen, M. S. Gordon, S. P. Webb, W. J. Stevens, M. Kraus, D. Garmer, H. Basch, and D. Cohen, J. Chem. Phys. **105**, 1968 (1996).
[4] J. H. Jensen and M. S. Gordon, Mol. Phys. **89**, 1313 (1996); J. H. Jensen and M. S. Gordon, J. Chem. Phys. **108**, 4772 (1998).
[5] A. J. Stone, Chem. Phys. Lett. **83**, 233 (1981).
[6] A. D. Buckingham, Quart. Rev. (London) **13**, 183 (1959).
[7] J. N. Murrell and J. J. C. Teixeira-Dias, Mol. Phys. **19**, 521 (1970).
[8] V. Kairys and J. H. Jensen, Chem. Phys. Lett. **315**, 140 (1999).
[9] J. H. Jensen, J. Chem. Phys. **104**, 7795 (1996).
[10] 1.0 kcal mol$^{-1}$=4.184 kJ mol$^{-1}$.
[11] B. T. Thole, Chem. Phys. **59**, 341 (1981).
[12] M. Krauss, D. B. Neumann, and W. J. Stevens, Chem. Phys. Lett. **66**, 29 (1979); A. Koide, J. Phys. B **9**, 3173 (1976); J. Hepburn, G. Scoles, and R. Penco, Chem. Phys. Lett. **36**, 451 (1975); R. Ahlrichs, P. Penco, and G. Scoles, Chem. Phys. **19**, 119 (1977).
[13] M. W. Schmidt, K. K. Baldridge, J. A. Boatz, S. T. Elbert, M. S. Gordon, J. H. Jensen, S. Koseki, N. Matsunaga, K. A. Nguyen, S. J. Su, T. L. Windus, M. Dupuis, and J. A. Montgomery, J. Comput. Chem. **14**, 1347 (1993).
[14] C. A. Coulson, Proc. Cambridge Philos. Soc. **38**, 222 (1942).
[15] A. D. Buckingham and P. W. Fowler, J. Chem. Phys. **79**, 6426 (1983); A. D. Buckingham and P. W. Fowler, Can. J. Chem. **63**, 2018 (1985).
[16] W. Chen and M. S. Gordon, J. Chem. Phys. **105**, 11081 (1996); P. N. Day and R. Pachter, *ibid.* **107**, 2990 (1997); G. N. Merrill and M. S. Gordon, J. Phys. Chem. **102**, 2650 (1998); C. P. Peterson and M. S. Gordon, *ibid.* **103**, 4146 (1999).